Vision Research 72 (2012) 55–62

Contents lists available at SciVerse ScienceDirect

Vision Research

journal homepage: www.elsevier.com/locate/visres

Perception of dynamic Glass patterns

Jean-François Nankoo *, Christopher R. Madan, Marcia L. Spetch, Douglas R. Wylie

Department of Psychology, University of Alberta, Edmonton, Alberta, Canada T6G 2E9

ARTICLE INFO

Article history:
Received 20 January 2012
Received in revised form 11 September 2012
Available online 24 September 2012

Keywords:
Glass pattern
Form perception
Motion perception
Random dot
Coherence threshold

ABSTRACT

In the mammalian brain, form and motion are processed through two distinct pathways at early stages of visual processing. However, recent evidence suggests that these two pathways may interact. Here we used dynamic Glass patterns, which have been previously shown to create the perception of coherent motion in humans, despite containing no motion coherence. Glass patterns are static stimuli that consist of randomly positioned dot pairs that are integrated spatially to create the perception of a global form, whereas dynamic Glass patterns consist of several independently generated static Glass patterns presented sequentially. In the current study, we measured the detection threshold of five types of dynamic Glass patterns and compared the rank order of the detection thresholds with those found for static Glass patterns and real motion patterns (using random dot stimuli). With both the static Glass patterns and dynamic Glass patterns, detection thresholds were lowest for concentric and radial patterns and highest for horizontal patterns. We also found that vertical patterns were better detected than horizontal patterns, consistent with prior evidence of a "horizontal effect" in the perception of natural scene images. With real motion, detection thresholds were equivalent across all patterns, with the exception of higher thresholds for spiral patterns. Our results suggest that dynamic Glass patterns are processed primarily as form prior to input into the motion system.

1. Introduction

Visual processing of form and motion is thought to be carried out independently by distinct neural substrates in the cortex of the mammalian brain (Braddick et al., 2000; Livingstone & Hubel, 1988; Milner & Goodale, 1995; Mishkin, Ungerleider, & Macko, 1983). Form information is processed in the ventral pathway, where information from V1 is carried to V4 and the inferior temporal cortex (IT). In contrast, motion information is processed by the dorsal pathway, where information from V1 is carried to the middle temporal area (MT) and to the parietal cortex. Support for this two-pathway hypothesis has come from numerous monkey and human lesion studies that have demonstrated that damage to the ventral pathway results in impairment of object recognition, whereas damage to the dorsal pathway results in impairment of motion processing (Livingstone & Hubel, 1988; Ungerleider & Mishkin, 1982). For instance, patient L.M., who had bilateral damage to the dorsal pathway, was found to exhibit an impairment in detecting visual motion but no impairment to other visual functions (e.g., object and face recognition; Zihl, Cramon, & Mai, 1983).

Despite the apparent segregation at the cortical level, psychophysical evidence suggests that there is an interaction of form and motion processing (see Kourtzi, Krekelberg, and van Wezel (2008) for review). For instance, 2D motion can provide 3D shape information, a phenomenon called structure-from-motion (Siegel & Andersen, 1988). Similarly, form information can also influence motion perception. As one example, trailing lines, i.e., motion streaks, behind fast moving objects have been shown to influence the perception of motion direction (Geisler, 1999). Further evidence that form influences motion processing was shown by Ross, Badcock, and Hayes (2000), who demonstrated that humans perceive coherent motion (termed "implied motion" by Krekelberg et al., 2003) when shown a rapid sequence of independently generated Glass patterns, termed "dynamic Glass pattern". Importantly, this occurs in spite of the fact that no coherent motion information is available in these patterns. A Glass pattern is a pattern that consists of an array of randomly placed dots that are each paired with a second dot oriented along a common rule (Glass, 1969; see Fig. 1). Given that each Glass pattern is generated based on an array of randomly placed dots, when a sequence of independently generated Glass patterns is shown, no coherent motion is present in the sequence. Ross, Badcock, and Hayes (2000) suggest that orientation information provided by the dipoles in Glass patterns influences motion perception in a similar way to motion streaks. Furthermore, Smith, Bair, and Movshon (2002) and Smith and Kohn (2007) showed that cells in V1 and V2 respond selectively to dipoles' orientation.

Krekelberg et al. (2003) and Krekelberg, Vatakis, and Kourtzi (2005) investigated the neural basis of dynamic Glass patterns in

* Corresponding author. Address: BS-P531 Biological Sciences Bldg., University of Alberta, Edmonton, Alberta, Canada T6G 2E9.
E-mail address: nankoo@ualberta.ca (J.-F. Nankoo).

0042-6989/$ - see front matter © 2012 Elsevier Ltd. All rights reserved.
http://dx.doi.org/10.1016/j.visres.2012.09.008

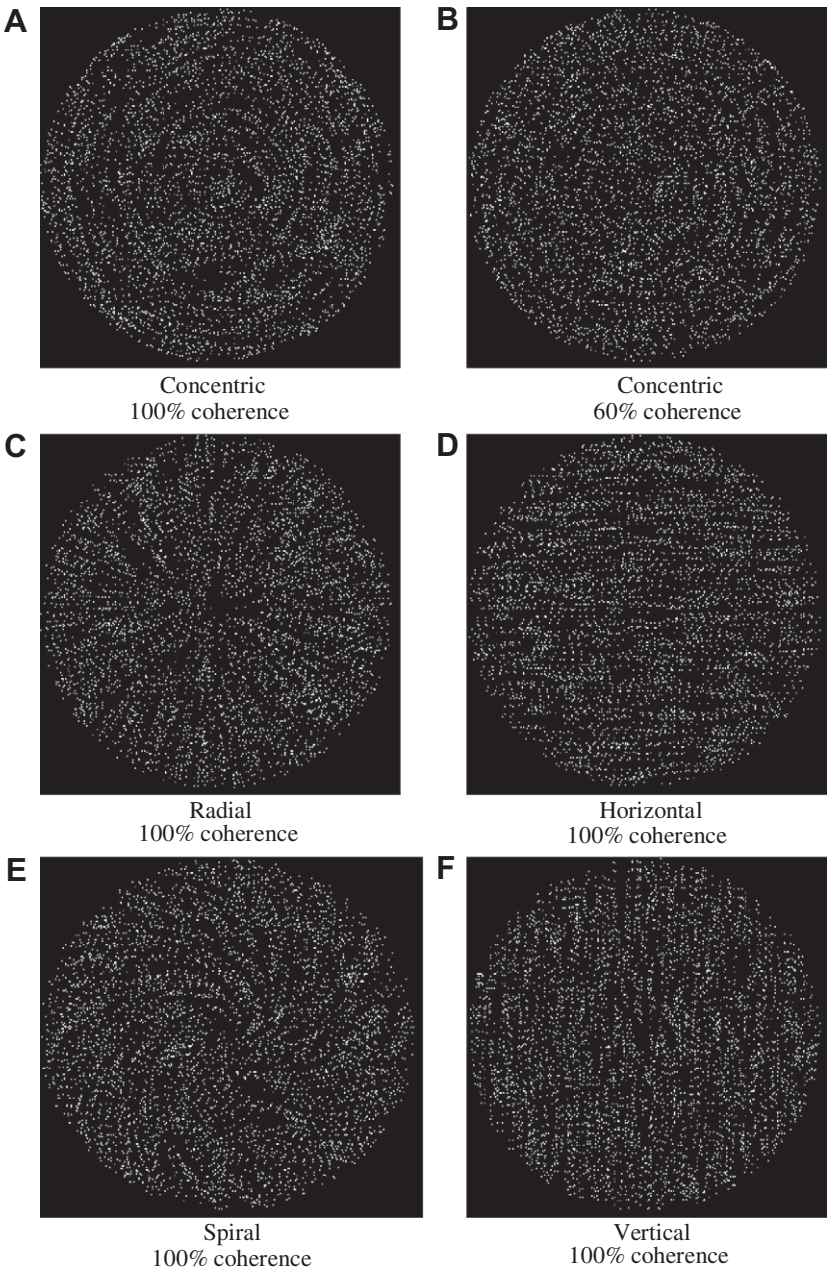

Fig. 1. Types of Glass patterns used in this study. Coherence (proportion of signal dots) was varied as illustrated with the concentric pattern at 60% coherence in panel B. In the real motion condition, each frame appeared as a random array of dots but the global motion pattern followed the same pattern as those of the Glass patterns.

monkeys and humans. Using single-unit recordings, Krekelberg et al. (2003) found that a subpopulation of motion selective cells in medial temporal (MT) and medial superior temporal (MST) areas of macaque monkeys did not differentiate between real coherent motion and dynamic Glass patterns. Krekelberg, Vatakis, and Kourtzi (2005) adapted this task into a human fMRI study and found similar results in the human visual cortex. Specifically, they found that the human motion complex (hMT+/V5) contains a subpopulation of cells that are selective to both implied motion (from dynamic Glass patterns) and real motion with the same pattern structure. In other words, these cells did not differentiate between real and implied motion. Krekelberg, Vatakis, and Kourtzi (2005) suggest that this overlap is why humans perceive coherent motion from the dynamic Glass patterns. Both implied and real motion have also been shown to be correlated with neural activation in the ventral pathway. However, in contrast to the areas in the dorsal pathway, in the ventral pathway, specifically in V4 and the lateral occipital complex (LOC), neurons that respond to implied motion patterns do not respond to real motion patterns and neurons that respond to real motion patterns do not respond to implied motion patterns.

Glass patterns are often used to investigate the processing of global form information because the shape of the patterns can only be determined by pooling the local information (Wilson & Wilkinson, 1998). Prior results have found that humans have different detection thresholds for different types of static Glass patterns, suggesting that the pooling mechanism is more efficient for certain types (Anderson & Swettenham, 2006; Aspell, Wattam-Bell, & Braddick, 2006; Kelly et al., 2001; Pei, Pettet, & Vildavski, 2005; Seu & Ferrera, 2001; Swettenham, Anderson, & Thai, 2010; Wilson & Wilkinson, 1998). Specifically, humans are usually more sensitive to concentric and radial forms (see Fig. 1A–C), as compared to

horizontal, vertical, and spiral forms (Fig. 1D–F). There is some debate over these results because Dakin and Bex (2002) observed an effect of the shape of the stimulus window on threshold, with sensitivity for concentric patterns being reduced when a square stimulus window is used. Other studies, however, have found greater sensitivity to concentric and radial over translational patterns even with a square window (Anderson & Swettenham, 2006; Kelly et al., 2001), suggesting that the window cannot account for the entire advantage shown by concentric or radial patterns. It is believed that form processing of translational patterns (i.e., horizontal and vertical patterns) likely occur at a local level whereas radial, concentric, and spiral are processed at a global level. In contrast, when using random dot motion stimuli (i.e., dots are coherently shifted across frames) to assess the thresholds for different types global coherent motion, humans do not show differential thresholds for radial, concentric, or translational motion (Blake & Aiba, 1998; Morrone, Burr, & Vaina, 1995). However, humans do exhibit a higher threshold for spiral motion (Morrone et al., 1999). It should be noted that recently Lee and Lu (2010) found that thresholds were lower for radial and circular compared to translational motion by using a multiple aperture stimulus using arrays of randomly oriented drifting Gabor elements. Lee and Lu (2010) suggest that the difference between their results and those using random dot stimuli may be a due to correspondence noise found in the random dot stimuli.

Currently it is known that people have a lower threshold for dynamic compared to static Glass patterns. Burr and Ross (2006) and Or, Khuu, and Hayes (2007) have reported that thresholds for concentric and translational dynamic Glass patterns were lower than the thresholds of equivalent static Glass patterns. However it is currently unclear whether detection thresholds for dynamic Glass patterns are lower because of their similarity to real motion patterns, and thus potentially reliant on motion-related processes, or whether the detection of dynamic Glass patterns is driven by the same mechanisms as static Glass patterns. In order to address this issue, we sought to measure the thresholds for different types of dynamic Glass patterns to determine whether the relative performance on each pattern type is similar to static Glass patterns or similar to real motion patterns. In the present study we measured the thresholds for five types of patterns (Fig. 1) and manipulated the presence or type of motion cue in three conditions: static Glass patterns, dynamic Glass patterns, and random dot stimuli that moved according to the types of pattern. In particular, the relative ranking of performance on each of the five patterns, across the three conditions, will indicate whether dynamic Glass patterns are encoded more similarly to real motion or to static forms. This is in turn will inform the research on form and motion interaction at an intermediate-level of visual processing.

2. Method

Seven adults with normal or corrected-to-normal vision participated in the static and dynamic Glass pattern conditions of this study ($n = 7$). This included all four authors, and three graduate students from the University of Alberta who had only cursory knowledge of the purpose of the experiment. Real motion consisted of the same participants with the exception of one author ($n = 6$). Prior to the actual experimental testing, the participants were given multiple training sessions and were therefore deemed to be experts in all three conditions.

2.1. Apparatus

Stimuli were displayed on a 19-in. Samsung SyncMaster 940BF monitor (resolution: 1280×1024 pixels; refresh rate: 60 Hz). Participants were seated comfortably at a viewing distance of 45 cm to the monitor, with the center of the monitor positioned at eye-level. Participants' head position was fixed with a chin rest.

Stimuli were generated in MATLAB (The MathWorks, Natick, MA) and saved as bitmap images. E-Prime version 2.0 (Psychology Software Tools Inc., Sharpsburg, PA) was used to present the stimuli and record responses.

2.2. Stimuli and design

Each stimulus was presented for a total duration of 167 ms. Five types of patterns were used in all the conditions (see Fig. 1). Each stimulus consisted of 10 frames of Glass patterns or random dot stimuli, each of which was updated at every monitor refresh (16.7 ms per frame). The method of constant stimuli was used to present the stimuli.

It should be noted that the dipole orientation for spiral Glass patterns was randomly angled to be either at 45° or 135°, midway between dipole orientations for radial (0°) and concentric (90°) patterns. For real motion, the angular displacement of signal dots for spiral motion was also randomly either 45° or 135°.

2.2.1. Static Glass patterns

Each Glass pattern subtended a visual angle of 11.16° and consisted of square dots with an angular size of $0.04° \times 0.04°$. The density of dots within each pattern was set at 6% and the dot separation was 0.26°. The 10 frames for this condition were identical Glass patterns, thus giving the appearance of being static. The coherence level was varied by changing the ratio of signal-to-noise dots within a pattern. The signal was defined as the amount of dipoles in the Glass pattern. Thus at 50%, only half of the dots in the Glass pattern were part of a dipole. A total of eight coherence levels were used: 0%, 20%, 30%, 40%, 50%, 60%, 80%, and 100%.

In addition to the five types of patterns, we included a control random pattern (Wilson & Wilkinson, 1998). The control random patterns consisted of dipoles oriented randomly (i.e., there was no global form). The coherence level of the control random pattern was also varied to match those of the other patterns by adjusting the number of dipoles.

2.2.2. Dynamic Glass patterns

These were the same as static Glass patterns with the exception that for each frame we presented a new independently generated Glass pattern (following from the same global rule).

In the case of spiral Glass patterns, all frames in a given trial consisted of the same type of spiral pattern (i.e., angular displacements of either 45° or 135°).

2.2.3. Real motion

The stimuli consisted of randomly placed dots in a circular display of the same size as the Glass patterns. The size and density of the dots were also the same as those of the Glass patterns. Each dot moved at a speed of 15.67°/s (i.e., the distance each dot shifted across frames was equivalent to the separation of Glass pattern dipoles, 0.26°, given that our image update rate was 60 Hz). Dots were removed when their position on the current frame reached the edge of the circular aperture. New dots were generated following from Gaussian probability functions, such that dots were most likely to be generated near the center of the circular aperture for spiral and radial patterns, but would be most likely to be generated near the starting edge of the motion for horizontal and vertical patterns (e.g., the top edge of the aperture for vertical patterns with downward motion). Note that in the concentric pattern, dots never exceeded the edge of the aperture and thus were never removed.

Patterns were generated such that the density of the pattern was consistently at 6%.

The image update rate, number of frames, and duration of stimuli were the same as those of static and dynamic Glass patterns. Five types of coherent motion were tested: concentric, radial, spiral, vertical and horizontal. Thus the motion patterns mimicked the form patterns used in static and dynamic Glass patterns conditions.

Coherence level was varied by changing the likelihood that a dot was a signal dot in each frame (i.e., we used a limited lifetime algorithm; Scase, Braddick, & Raymond, 1996). Signal dots moved in the coherent direction, whereas noise dots moved randomly (distance and direction). At 100% coherence, each dot has a 100% chance of being chosen as a signal dot, and therefore all the dots move coherently. However, at 50% coherence, on each frame each dot has a 50% chance of being a signal dot. The coherence levels in this condition were 0%, 20%, 30%, 40%, 50%, 60%, 80%, and 100%. However, due to the fact that motion was easily detected for all patterns except for spiral (i.e., performance was near-ceiling at coherences of 20%), we conducted an additional session using coherence levels of 0%, 4%, 6%, 8%, 10%, 12%, 16%, and 20% to obtain more precise threshold estimates.

The direction of motion within a trial remained consistent across frames, but was counterbalanced within the session. For radial patterns, the direction of motion moved inward (i.e., contraction) on half of the trials and outward (i.e., expansion) on half of the trials. These motion patterns were pre-generated such that dots always moved outwards (i.e., expansion). To create motion patterns where dots moved inwards (i.e., contraction), frame sequences were simply presented in the reverse order relative to how they were initially generated. Concentric patterns rotated either clockwise or counterclockwise; horizontal patterns moved left or right; vertical patterns moved up or down; spiral patterns rotated inward-clockwise or outward-counterclockwise.

2.3. Procedure

At the beginning of each block of trials, participants were told which type of pattern they would be trying to detect. As illustrated in Fig. 2, the participants began the trial by clicking a yellow start stimulus. The stimulus display was then presented, followed by the appearance of two response circles. The green response circle always appeared on the left side of the screen, along with the word "Pattern", while the red circle always appeared on the right side of the screen, along with the words "No Pattern". Participants selected the green circle with the computer mouse if they perceived a coherent pattern, otherwise they selected the red circle. After the participant responded, there was a 250 ms delay before the yellow start stimulus appeared to begin the next trial.

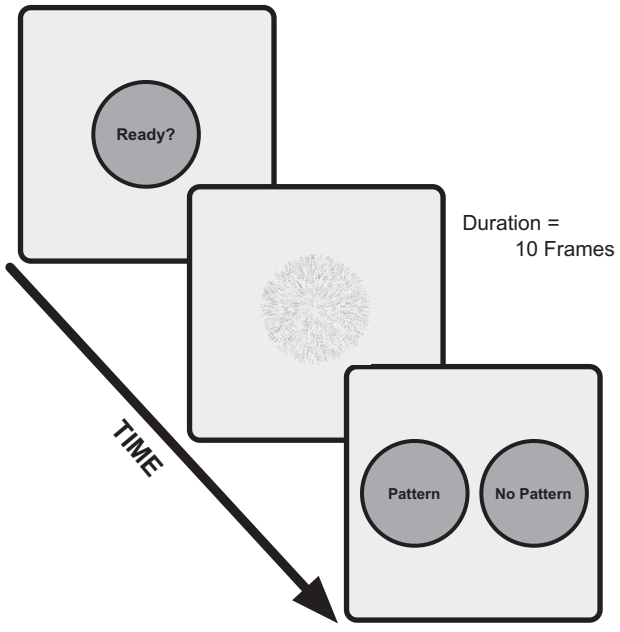

Fig. 2. Illustration of a single trial. Polarity of the pattern is reversed for illustrative purposes only. In the experiment the participants viewed white dots on a black background, as in Fig. 1.

Testing was carried out in five blocks: one block for each type of pattern. In each condition, a total of 20 trials per coherence level were presented for both the given pattern and the random control. This yielded a total of 320 trials within a block. Participants were allowed to take a brief break between blocks but were required to complete all five blocks in a single day.

2.4. Data analysis

To analyze the data, we first calculated the proportion of responses for which the participant detected a pattern at each coherence level (i.e., hits), for each block. We also calculated the proportion of responses for which the participant detected a pattern for random stimuli at each coherence level (i.e., false alarms). We then calculated d', following from standard signal-detection analyses (Green & Swets, 1966), by finding the difference of the Z-transformed values for hits and false alarms. We then plotted the d' values as a function of coherence level (Fig. 3).

Participants' coherence threshold for each pattern was estimated using a three-parameter cumulative Weibull function (Weibull, 1951), $F(c)$, of the following form:

$$F(c) = \alpha(1 - e^{-(c/\beta)^{\gamma}})$$

where c is the coherence level, and α, β, and γ are the asymptote, spread, and shape parameters, respectively. The Weibull function was fit to data for each pattern, for each participant, by means of the Nelder and Mead (1965) simplex algorithm set to minimize the root-mean-squared-deviation (RMSD) between the function's estimation and the data. This procedure was repeated for 1000 iterations to ensure the global minima was found. The threshold was then calculated as the coherence level corresponding to $d' = 1.5$, using the best-fitting parameters.

All statistical analyses were conducted using SigmaPlot (Systat Software Inc., Chicago, IL) and MATLAB (The MathWorks Inc., Natick, MA). Effects were considered significant based on an alpha level of .05.

One-way repeated-measures ANOVAs and Tukey post hoc pairwise analyses were conducted on the log-transformed threshold coherence levels of the different patterns. If the data violated the assumptions for parametric tests, a non-parametric test (Kruskal–Wallis) was performed instead, with pairwise comparisons conducted using Dunn's method. We then calculated the standard error for each pattern across participants before exponentially transforming the threshold back for reporting.

3. Results

3.1. Static Glass patterns

The mean d' for each pattern is plotted as a function of coherence level in Fig. 3A. Fig. 3B shows the mean coherence threshold of each pattern. A one-way repeated-measures ANOVA yielded a significant effect of pattern type, $F(4, 24) = 21.72$, $p < .001$. Tukey post hoc analyses demonstrated that the thresholds for concentric and radial patterns were significantly lower than the thresholds of the other patterns (all $ps < .05$) but did not differ from each other

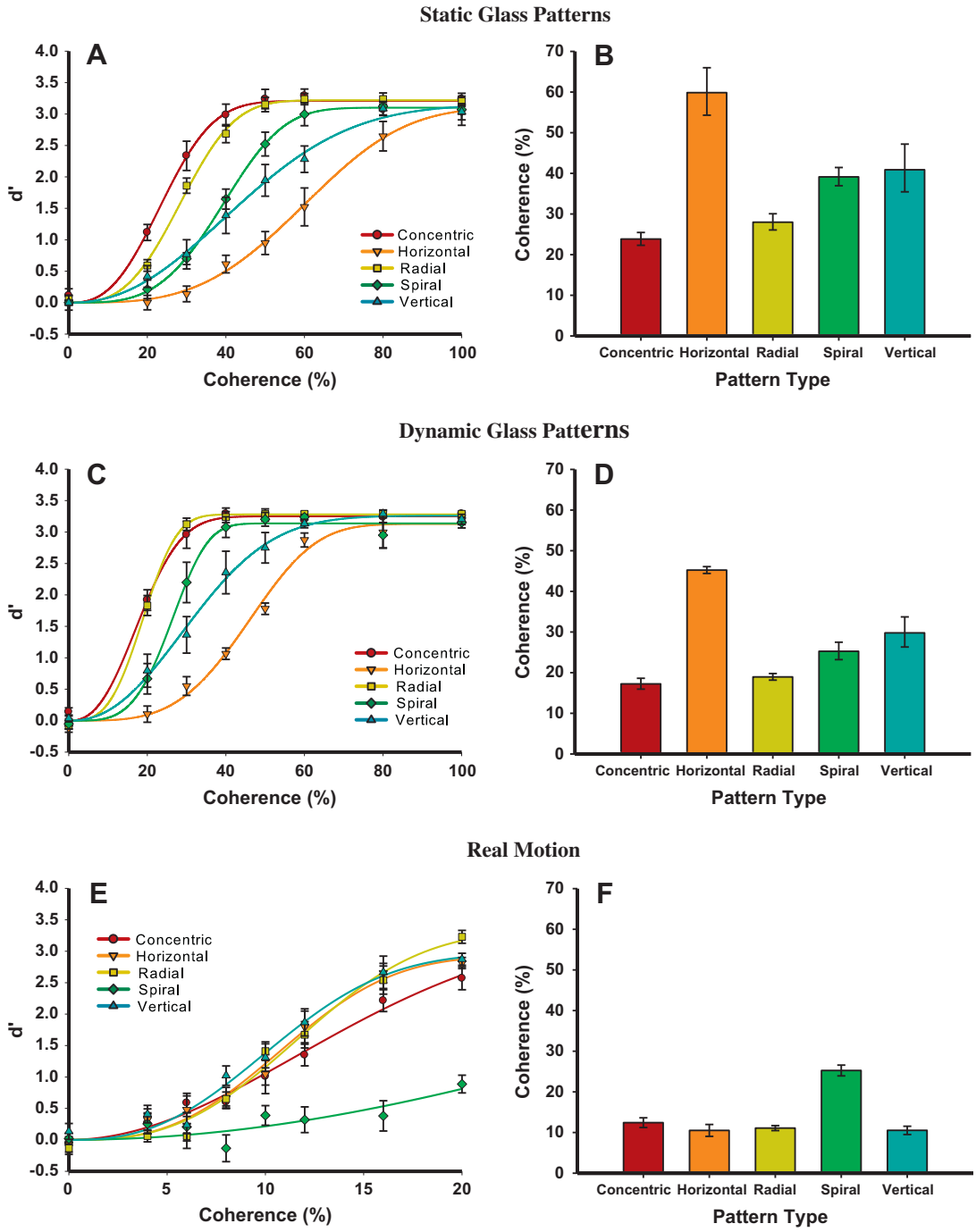

Fig. 3. Panels A, C, and E represent the d' as a function of coherence level for each pattern type, within each condition. Lines represent the Weibull function fit for each pattern type; markers represent the observed d'. Panels B, D, and F represent the threshold (coherence level corresponding to a d' of 1.5) for each pattern type, within each condition. Error bars represent the standard error of the mean.

($p > .1$). The threshold for spiral patterns was significantly lower than for horizontal patterns ($p < .01$) but not different from the threshold for vertical patterns ($p > .1$). Finally, the threshold for vertical patterns was significantly lower than the threshold for horizontal patterns ($p < .05$).

3.2. Dynamic Glass patterns

The mean d' for each pattern was plotted as a function of coherence level and is shown in Fig. 3C. Fig. 3D shows the mean threshold estimates for each pattern. As with the static Glass patterns, a one-way repeated-measures ANOVA revealed a significant effect of pattern type, $F(4, 24) = 21.75$, $p < .001$. Tukey post hoc analyses found that thresholds for concentric and radial patterns did not differ from each other ($p > .1$) but were significantly lower than the thresholds for vertical and horizontal patterns (all $ps < .05$). The threshold for concentric patterns was lower than for spiral ($p < .05$); the threshold for radial did not differ to that for spiral ($p > .1$). The threshold for spiral pattern was also not different from the threshold for vertical patterns ($p > .1$), but was significantly

lower than for horizontal patterns ($p < .001$). The threshold for vertical patterns was also found to be significantly lower than for horizontal ($p < .01$).

In addition to the above results, it should be noted that none of the participants reported seeing a reversal of directions within a trial.

3.3. Real motion

The mean d' for each pattern was plotted as a function of coherence level and is shown in Fig. 3E. Fig. 3F shows the mean threshold estimates for each pattern of motion. The results of a one-way repeated-measures ANOVA showed a significant effect of pattern type, $F(4,20) = 30.55$, $p < .001$. Tukey post hoc analyses revealed that there were no significant differences in threshold for concentric, radial, vertical, and horizontal motion (all $ps > .05$). However, the threshold for spiral motion was significantly higher than for each of the other patterns (all $ps < .001$).

Paired t-tests were used to compare the log-transformed thresholds between the two directions of motion in each pattern (e.g., radial motion: inward vs. outward, vertical: up vs. down). We found no significant difference in thresholds between motion directions for radial, concentric, horizontal, and vertical (all $ps > .05$; Bonefferoni corrected). However, this difference was significant for spiral, with participants detecting inward-clockwise motion with lower thresholds than outward-counterclockwise motion ($p < .05$; Bonefferoni corrected).

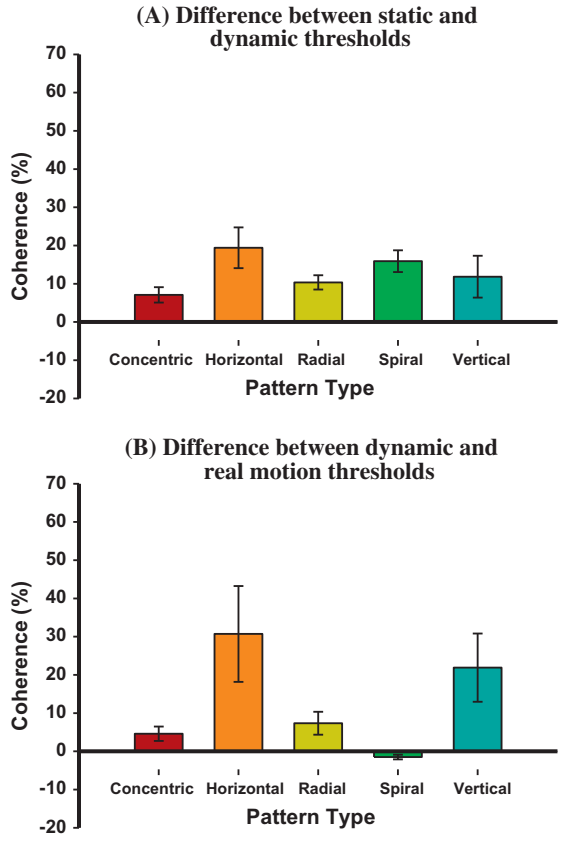

Fig. 4. Panel A shows the mean difference between the threshold for each pattern in the static Glass pattern condition and the dynamic Glass pattern condition. Panel B shows the mean difference between the threshold for each pattern in the dynamic Glass pattern condition and the real motion condition.

3.4. Effect of motion

There was a significant difference in the general performance (i.e., mean log-transformed threshold across patterns) between static Glass patterns (*median* = 3.53), dynamic Glass patterns (*median* = 3.14), and real motion (*median* = 2.49), $H(2) = 50.26$, $p < .001$. Pairwise analyses revealed that performance in real motion was significantly better than performance in for both static Glass patterns and the dynamic Glass patterns (both $ps < .05$). Performance in the dynamic Glass patterns was also found to be significantly better compared to performance in the static Glass patterns ($p < .05$) (see Fig. 4).

4. Discussion

Coherence thresholds for different patterns of implied motion (i.e., motion coherence generated by form cues) were determined using dynamic Glass patterns and then contrasted with thresholds for comparable static Glass patterns and patterns of real motion (using random dot stimuli). We found that even though humans perceive dynamic Glass patterns as coherent motion (also see Ross, Badcock, & Hayes, 2000), dynamic Glass patterns appear to be processed more similarly to static Glass patterns than to real motion. Specifically, we found that with both static and dynamic Glass patterns, our participants were more sensitive to concentric and radial patterns than to the other patterns. Furthermore, we found that our participants were better at detecting vertical patterns compared to horizontal patterns with both dynamic and static Glass patterns. In contrast, with real motion we found no significant differences in participants' ability to detect concentric, radial, vertical, and horizontal patterns, consistent with previous findings (Morrone, Burr, & Vaina, 1995; but see Lee & Lu, 2010). Additionally, participants were worst at detecting spiral motion pattern in real motion (also see Morrone et al., 1999), despite detecting spiral patterns relatively well in both static and dynamic Glass patterns.

The consistent detection threshold rankings across the patterns for dynamic and static Glass patterns suggests that in both cases participants may have been engaging in a form detection task (i.e., they based their decision on individual frames). However, given that thresholds were significantly lower for dynamic Glass patterns than for static patterns, it seems unlikely that participants simply based their judgement on the static form of one particular frame in the implied motion condition. If this were the case, the detection thresholds, in addition to the threshold ranking across patterns, should be equivalent in dynamic and static Glass patterns. Instead, our findings indicate that the detection of dynamic Glass patterns likely relies on a summation process where stimulus information is integrated across the ten frames of independent Glass patterns. That is, the signal in dynamic Glass pattern may be amplified due to summation across the ten independent Glass patterns. This potential temporal summation in the form areas then strongly influences the coherence thresholds in implied motion. It should be noted that given the lower detection thresholds across *all* pattern types, our results serve as evidence of a local-level summation process. However, our results do not exclude the possibility that summation also occurs at the level of global detectors.

The results of our study suggest that the improved performance observed in dynamic Glass patterns may be due to the fact that multiple signals (form cues) were being presented. The improved performance that we observed in the dynamic Glass pattern conditions is reminiscent of improved behavioral performance due to repetition of images with complementary parts (i.e., perceptual priming) (Biederman & Cooper, 1991; see Grill-Spector, Henson, and Martin (2006), Wiggs and Martin (1998) and Henson (2003)

for reviews on perceptual priming). Moreover, our results are also in congruence with the findings from Beintema and Lappe (2002), who found that people are able to identify biological motion from a sequence of positional cues. In this study, Beintema and Lappe eliminated the role of motion signals by positioning the light points on the limbs rather than the joints and randomly relocating them on each frame. This result is also supported by studies finding that patients with lesioned motion areas are still able to perceive biological motion (Mcleod et al., 1996; Vaina et al.,1990). In a quantitative model of biological motion, Giese and Poggio (2003) suggest that "snapshot" neurons in the ventral pathway code for body shapes, and subsequently motion pattern neurons summate sequences of body shapes from the activity of these snapshot neurons. Our results suggest that a similar process likely occurs in the perception of dynamic Glass patterns, where form information from multiple frames can temporally summate in the absence of real motion cues.

Furthermore, we observed a difference in the ranking of the thresholds between dynamic Glass patterns and real motion patterns. This difference, along with the similarity between the ranking of the threshold between dynamic and static Glass patterns, indicates that dynamic Glass patterns are processed for their global form and then subsequently processed in the motion system. Supporting this conclusion, Krekelberg, Vatakis, and Kourtzi (2005) found that the same subpopulations of neurons are selective for implied and real motion patterns in hMT+/V5 (prototypical motion area). If implied motion was processed by MT+/V5 independently of global form areas, thresholds for implied motion should match those found with real motion. However, even when we lowered the coherence levels for real motion, this was not the case. Thus, it is likely that V4 and the LOC (areas suggested to be involved in extracting global form; Gallant, Shoup, & Mazer, 2000; Krekelberg, Vatakis, & Kourtzi, 2005; Ostwald et al., 2008) extract form information from dynamic Glass patterns and pass these signals to MT+/V5. This notion is further supported by Krekelberg, Vatakis, and Kourtzi's (2005) finding that neurons responsive for real motion were not selective for implied motion in the ventral pathway. Taken together, our findings, in conjunction with those from Krekelberg, Vatakis, and Kourtzi (2005), suggest that global form may be fully processed and subsequently influence activation in motion regions.

We additionally found that the sensitivity to vertical Glass patterns was significantly greater than that to horizontal Glass pattern, not only for static stimuli but also for dynamic Glass patterns. This difference has previously been reported in the detection of static Glass patterns (Kelly et al., 2001). This anisotropy may be due to what is known as the horizontal effect (Essock et al., 2003). The horizontal effect is found in broadband stimuli where observers are relatively worse at perceiving horizontal stimuli than vertical and oblique stimuli. Hansen and Essock (2004) suggest that the horizontal effect is the result of the visual system discounting orientation information that is more dominant in natural images, most notably horizontally oriented information. Supporting the generalization of this effect to Glass patterns, Wilson et al. (2001) found that humans have a lower threshold for oblique Glass patterns compared to horizontal and vertical Glass patterns. Given that oblique contents are less prevalent compared to horizontal and vertical in natural scenes (Hansen & Essock, 2004) these results provide further support for the hypothesis of a horizontal effect in complex stimuli. It should also be noted that the differences between horizontal and vertical stimuli are also supported by recent fMRI results that found that an array of horizontal and vertical line segments activate different cortical areas beyond V1 (Aspell et al., 2010). Importantly, the results of the current study are the first evidence of this difference in the detection of dynamic Glass patterns.

In conclusion, we have found that the ranking of thresholds for different types of implied motion generated by dynamic Glass patterns are similar to those found for static Glass patterns. This suggests that in spite of a strong coherent motion illusion, dynamic Glass pattern appear to be processed first primarily as form information prior to being input into the motion system. This hypothesis is further strengthened by the result of a horizontal effect in both static and dynamic Glass pattern, but not with real motion.

Acknowledgments

This research was supported by grants from the National Science and Engineering Research Council (NSERC) of Canada to M.L.S and D.R.W. We are grateful to Alinda Friedman and Quoc Vuong for their feedback, as well as three graduate students at the University of Alberta who were participants in the experiment (M.K.M., N.E.H., Y.Y.C.).

References

Anderson, S. J., & Swettenham, J. B. (2006). Neuroimaging in human amblyopia. *Strabismus, 14*, 21–35.
Aspell, J. E., Wattam-Bell, J., Atkinson, J., & Braddick, O. J. (2010). Differential human brain activation by vertical and horizontal global visual textures. *Experimental Brain Research, 202*, 669–679.
Aspell, J. E., Wattam-Bell, J., & Braddick, O. (2006). Interaction of spatial and temporal integration in global form processing. *Vision Research, 46*, 2834–2841.
Beintema, J. A., & Lappe, M. (2002). Perception of biological motion without local image motion. *Proceedings of the National Academy of Sciences of the United States of America, 99*, 5661–5663.
Biederman, I., & Cooper, E. E. (1991). Priming contour-deleted images: Evidence for intermediate representations in visual object recognition. *Cognitive Psychology, 23*, 393–419.
Blake, R., & Aiba, T. S. (1998). Detection and discrimination of optical flow components. *Japanese Psychological Research, 40*, 19–30.
Braddick, O. J., O'Brien, J. M., Wattam-Bell, J., Atkinson, J., & Turner, R. (2000). Form and motion coherence activate independent, but not dorsal/ventral segregated, networks in the human brain. *Current Biology, 10*, 731–734.
Burr, D., & Ross, J. (2006). The effects of opposite-polarity dipoles on the detection of Glass patterns. *Vision Research, 46*, 1139–1144.
Dakin, S. C., & Bex, P. J. (2002). Summation of concentric orientation structure: Seeing the Glass or the window? *Vision Research, 42*, 2013–2020.
Essock, E., DeFord, J. K., Hansen, B. C., & Sinai, M. J. (2003). Oblique stimuli are seen best (not worst!) in naturalistic broad-band stimuli: A horizontal effect. *Vision Research, 43*, 1329–1335.
Gallant, J. L., Shoup, R. E., & Mazer, J. A. (2000). A human extrastriate area functionally homologous to macaque V4. *Neuron, 27*, 227–235.
Geisler, W. S. (1999). Motion streaks provide a spatial code for motion direction. *Nature, 400*, 65–69.
Giese, M. A., & Poggio, T. (2003). Neural mechanisms for the recognition of biological movements. *Nature Reviews Neuroscience, 4*, 179–192.
Glass, L. (1969). Moire effect from random dots. *Nature, 223*, 578–580.
Green, D. M., & Swets, J. A. (1966). *Signal detection theory and psychophysics*. New York: Wiley.
Grill-Spector, K., Henson, R., & Martin, A. (2006). Repetition and the brain: Neural models of stimulus-specific effects. *Trends in Cognitive Sciences, 10*, 14–23.
Hansen, B. C., & Essock, E. A. (2004). A horizontal bias in human visual processing of orientation and its correspondence to the structural components of natural scenes. *Journal of Vision, 4*, 1044–1060.
Henson, R. N. (2003). Neuroimaging studies of priming. *Progress in Neurobiology, 70*, 53–81.
Kelly, D. M., Bischof, W. F., Wong-Wylie, D. R., & Spetch, M. L. (2001). Detection of glass patterns by pigeons and humans: Implications for differences in higher-level processing. *Psychological Science, 12*, 338–342.
Kourtzi, Z., Krekelberg, B., & van Wezel, R. J. A. (2008). Linking form and motion in the primate brain. *Trends in Cognitive Sciences, 12*, 230–236.
Krekelberg, B., Dannenberg, S., Hoffmann, K. P., Bremmer, F., & Ross, J. (2003). Neural correlates of implied motion. *Nature, 424*, 674–677.
Krekelberg, B., Vatakis, A., & Kourtzi, Z. (2005). Implied motion from form in the human visual cortex. *Journal of Neurophysiology, 94*, 4373–4386.
Lee, A. L. F., & Lu, H. (2010). A comparison of global motion perception using a multiple-aperture stimulus. *Journal of Vision, 10*, 1–16.
Livingstone, M., & Hubel, D. (1988). Segregation of form, color, movement, and depth: Anatomy, physiology, and perception. *Science, 240*, 740–749.
Mcleod, P., Dittrich, W., Driver, J., Perrett, D., & Zihl, J. (1996). Preserved and impaired detection of structure from motion by a "Motion-blind" patient. *Visual Cognition, 3*, 363–391.
Milner, A. D., & Goodale, M. A. (1995). *The visual brain in action*. Oxford: Oxford University Press.

Mishkin, M., Ungerleider, L. G., & Macko, K. A. (1983). Object vision and spatial vision: Two cortical pathways. *Trends in Neurosciences, 6*, 414–417.
Morrone, M. C., Burr, D. C., Di Pietro, S., & Stefanelli, M. A. (1999). Cardinal directions for visual optic flow. *Current Biology, 9*, 763–766.
Morrone, M., Burr, D. C., & Vaina, L. M. (1995). Two stages of visual processing for radial and circular motion. *Nature, 376*, 507–509.
Nelder, J. A., & Mead, R. (1965). A simplex method for function minimization. *Computer Journal, 7*, 308–313.
Or, C. C.-F., Khuu, S. K., & Hayes, A. (2007). The role of luminance contrast in the detection of global structure in static and dynamic, same- and opposite-polarity, Glass patterns. *Vision Research, 47*, 253–259.
Ostwald, D., Lam, J. M., Li, S., & Kourtzi, Z. (2008). Neural coding of global form in the human visual cortex. *Journal of Neurophysiology, 99*, 2456–2469.
Pei, F., Pettet, M., & Vildavski, V. (2005). Event-related potentials show configural specificity of global form processing. *Neuroreport, 16*, 1427–1430.
Ross, J., Badcock, D. R., & Hayes, A. (2000). Coherent global motion in the absence of coherent velocity signals. *Current Biology, 10*, 679–682.
Scase, M. O., Braddick, O. J., & Raymond, J. E. (1996). What is noise for the motion system? *Vision Research, 36*, 2579–2586.
Seu, L., & Ferrera, V. (2001). Detection thresholds for spiral Glass patterns. *Vision Research, 41*, 3785–3790.
Siegel, R., & Andersen, R. (1988). Perception of three-dimensional structure from motion in monkey and man. *Nature, 331*, 259–261.
Smith, M. A., Bair, W., & Movshon, J. A. (2002). Signals in macaque striate cortical neurons that support the perception of glass patterns. *Journal of Neuroscience, 22*, 8334–8345.
Smith, M., & Kohn, A. (2007). Glass pattern responses in macaque V2 neurons. *Journal of Vision, 7*, 1–15.
Swettenham, J. B., Anderson, S. J., & Thai, N. J. (2010). MEG responses to the perception of global structure within glass patterns. *PloS One, 5*, e13865.
Ungerleider, L. G., & Mishkin, M. (1982). Two cortical visual systems. In D. J. Ingle, M. A. Goodale, & R. J. W. Mansfield (Eds.), *Analysis of visual behavior* (pp. 549–586). Cambridge: MIT Press.
Vaina, L., Lemay, M., Bienfang, D., Choi, A., & Nakayama, K. (1990). Intact "biological motion" and "structure from motion" perception in a patient with impaired motion mechanisms: A case study. *Visual Neuroscience, 5*, 353–369.
Weibull, W. (1951). A statistical distribution function of wide applicability. *Journal of Applied Mechanics, 18*, 292–297.
Wiggs, C. L., & Martin, A. (1998). Properties and mechanisms of perceptual priming. *Current Opinion in Neurobiology, 8*, 227–233.
Wilson, H. R., Loffler, G., Wilkinson, F., & Thistlethwaite, W. A. (2001). An inverse oblique effect in human vision. *Vision Research, 41*, 1749–1753.
Wilson, H. R., & Wilkinson, F. (1998). Detection of global structure in Glass patterns: Implications for form vision. *Vision Research, 38*, 2933–2947.
Zihl, J., Cramon, D. V., & Mai, N. (1983). Selective disturbance of movement after bilateral brain damage. *Brain, 106*, 313–340.